THE HII REGIONS AND BOW SHOCKS AROUND RUNAWAY O STARS

A. C. Raga[1], J. Cantó[2], and A. Noriega-Crespo[3]

ABSTRACT

We present a model for the HII region and stellar wind bow shock formed by runaway O stars passing through the Galactic disk. We develop a quasi-analytic approach in which the absorption of stellar ionizing photons by the bow shock is considered. With these models we study the transition between a detached ionization front (leading the bow shock) and an ionization front trapped by the stellar wind bow shock. We find that for an O7 star one needs to have a stellar velocity of only a few km/s and an environmental density $> 10^5$ cm^{-3}.

RESUMEN

Presentamos un modelo para la región HII y para el choque de proa del viento estelar producidas por estrellas O fugadas pasando a través del plano galáctico. Desarrollamos un modelo cuasi-analítico que incluye la absorción de los fotones ionizantes estelares por el choque de proa. Con estos modelos estudiamos la transición entre un frente de ionización libre (que precede al choque de proa) y un frente de ionización atrapado por el choque de proa. Encontramos que para una estrella O7 se necesita una velocidad estelar de unos pocos km/s y una densidad ambiental $> 10^5$ cm^{-3}.

Key Words: HII regions — hydrodynamics — stars: winds, outflows

1. INTRODUCTION

Runaway O stars pass through the Galactic disk at velocities of ≈ 100 km s^{-1} (see, e.g., Cruz-González et al. 1974). These stars interact with the interstellar medium of the disk, forming an inner stellar wind bow shock, and an outer "cometary" HII region. Observations of these structures are presented, e.g., by Van Buren et al. (1995) and Noriega-Crespo et al. (1997). We note that these HII regions have a somewhat elongated "tear-drop" shape, and that the "cometary" label that is applied to them is somewhat misleading.

The problem of the cometary HII region for a star in hypersonic motion was solved analytically by Rasiwala (1969) and numerically by Thuan (1975). Axisymmetric gasdynamic simulations of this flow were presented by Raga et al. (1997).

The standard, ram-pressure balance stellar wind bow shock has the well used analytic solution of Dyson (1975). Also, at a somewhat surprisingly later time, an analytic solution to the full, thin shell stellar wind bow shock problem (including the "centrifu-

gal pressure") was found (Wilkin 1996; Cantó et al. 1996). The stellar wind bow shock problem has been studied extensively with gasdynamic numerical simulations (see, e.g., Stevens et al. 1992).

Stellar wind bow shock models have been used to model compact/ultracompact HII regions formed by young O stars within molecular clouds (e.g., Van Buren 1990; Mac Low 1991), moving at velocities of a few km/s through the surrounding cloud. The models for these objects generally assume that the ionization front is trapped within the stellar wind bow shock, so that the flow differs from the detached bow shock/HII region found in runaway O stars. Gasdynamic simulations of bow shock compact HII regions have been presented by Arthur & Hoare (2006).

Simulations of bow shocks around runaway stars have been computed including thermal conduction (Meyer et al. 2014) and magnetic fields (Meyer et al. 2017). The cometary HII regions surrounding these bow shocks have been modeled in detail (in axisymmetry and 3D, including an environmental magnetic field) by Mackey et al. (2013). Interestingly, even in the work of Raga et al. (1997), which modeled both the bow shock and the cometary HII region of runaway O stars, these two structures of the flow have

[1]Instituto de Ciencias Nucleares, UNAM, México.
[2]Instituto de Astronomía, UNAM, México.
[3]STScI.

been considered separately. In the present paper we explore the regime in which the bow shock, while not trapping the ionization front, produces a substantial absorption of the stellar ionizing photons, therefore modifying the surrounding HII region.

We describe the flow by considering the thin shell analytic solution (of Wilkin 1996; Cantó et al. 1996 and Cantó et al. 2005) for the stellar wind bow shock. A review of this solution is presented in §2. We then write a modified form for the equation of Rasiwala (1969) and Raga et al. (1997), including the absorption of ionizing photons by the bow shock (§ 3) and integrate it numerically to obtain the self-consistent HII region+bow shock solution for a set of parameters (§ 4). Finally, in the summary (§ 5) we diScuss the possible application of the new model for the case of compact/ultracompact HII regions, and the further steps that will be necessary to study the full parameter space of these objects.

2. THE BOW SHOCK

A star with an isotropic wind of mass loss rate $\dot{M}_w$ and (terminal) wind velocity v_w moving hypersonically at a velocity v_a through a uniform medium of density ρ_a produces a double bow shock (with one shock stopping the wind and the second shock pushing the environment). This is shown schematically in Figure 1, as seen in a reference system moving with the star.

Wilkin (1996) and Cantó et al. (1996) found an analytic solution for the steady, thin shell stellar bow shock problem:

$$R_b(\theta) = R_0 \csc\theta\sqrt{3(1 - \theta\,\mathrm{ctg}\,\theta)}\,, \qquad (1)$$

with

$$R_0 \equiv \sqrt{\frac{\dot{M}_w v_w}{4\pi\rho_a v_a^2}}\,, \qquad (2)$$

and where the polar angle θ and the spherical radius R_b are shown in Figure 1.

Interestingly, the axisymmetric gasdynamic simulations of Raga et al. (1997) show that even though the bow shock driven by a runaway O star has a complex, time-dependent structure and a separation of $\approx 0.3R_0$ between the two bow shocks, it still approximately follows the thin shell solution of equation (1). We therefore adopt this thin shell solution as a valid description of the stellar wind bow shock.

We also use the emission measure:

$$EM = \int_0^h n^2 dl\,, \qquad (3)$$

i.e., the square of the ion number density ($n = \rho/\overline{m}$ for fully ionized H and singly ionized He) integrated
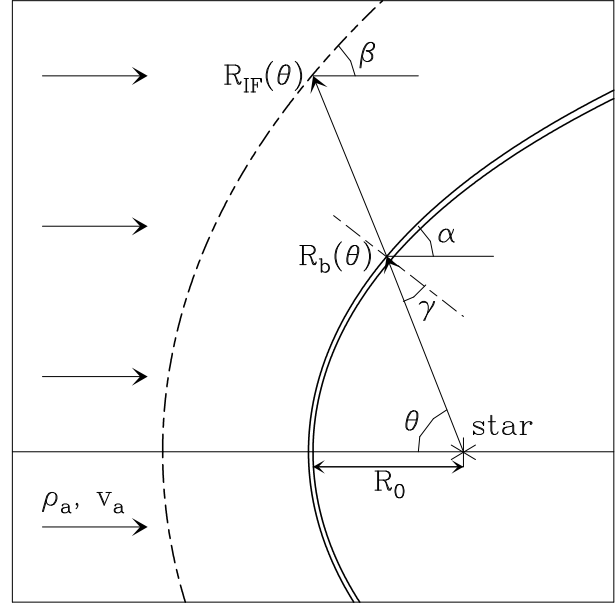

Fig. 1. Schematic diagram showing a star with an isotropic wind interacting with a uniform, streaming environment (of density ρ_a and velocity v_a). A two-shock stellar wind bow shock with a locus $R_b(\theta)$ (two thick, solid curves) and a detached ionization front of locus $R_{IF}(\theta)$ (thick, dashed curve) are formed. The angles θ, α and γ (used in the derivation of the model equations) are shown.

across the width h of the thin shell. This integral was calculated by Cantó et al. (2005) for a bow shock travelling into an environment with a density gradient, and their results can be used (by setting the density gradient to zero) to obtain the emission measure for a bow shock in a uniform environment:

$$EM = EM_0 \left[f_a(\theta) + f_w(\theta)\right] g_\sigma(\theta)\,, \qquad (4)$$

with

$$EM_0 = \frac{\rho_a v_a v_w}{2\overline{m}^2 c_0^2}\left(\frac{\dot{M}_w \rho_a}{4\pi v_w}\right)^{1/2}\,, \qquad (5)$$

where $\overline{m} = 1.3$ m_H for gas with 0.9 H and 0.1 He number abundance, $c_0 \approx 10$ km s^{-1} is the sound speed of the photoionized gas, and $f_a(\theta)$, $f_w(\theta)$ and $g_\sigma(\theta)$ are given in Appendix A.

3. THE EQUATION FOR THE HII REGION

For a star that emits S_* ionizing photons per unit time, if the bow shock shell does not trap the ionization front, we will have a cometary HII region surrounding the stellar wind bow shock (see the schematic diagram of Figure 1). For a hypersonic flow, the ionization front limiting this HII region will not produce a hydrodynamic perturbation, and the
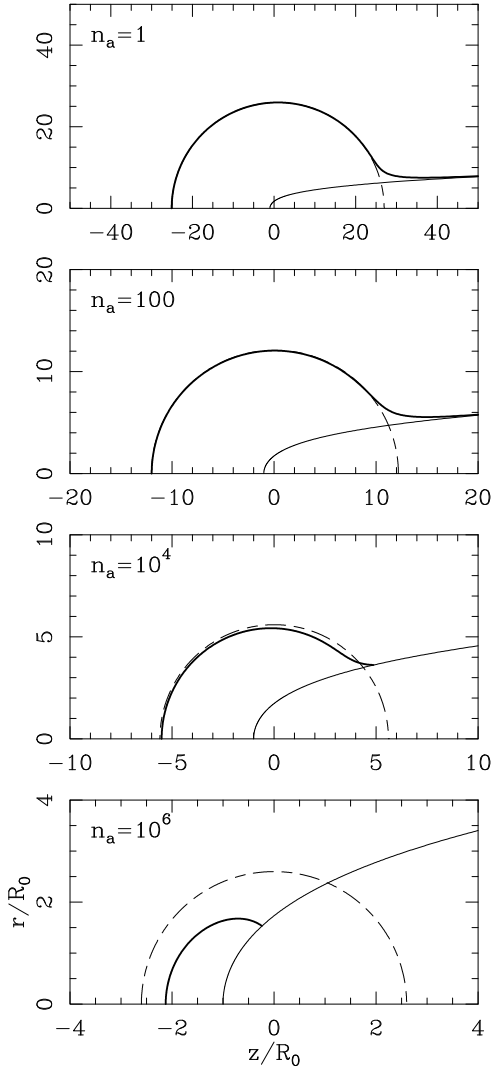
Fig. 2. The ionization front (thick, solid outer curve) and the stellar wind bow shock (thin, solid inner curve) obtained for models with $v_a = 20\,\mathrm{km\,s}^{-1}$ and $n_a = 1$ (top frame), 100, 10^4 and 10^6 cm^{-3} (bottom). The dashed curves show the ionization front that would be obtained for a star with no wind. The (z, r) axes are given in units of R_0.

environmental material will therefore flow with density ρ_a and velocity v_a until it intercepts the bow shock (see Figure 1).

The equation determining the locus $R_{IF}(\theta)$ of the ionization front is:

$$\frac{2\pi}{3} \sin\theta \left(R_{IF}^3 - R_b^3 \right) n_a^2 \alpha_H + n_a v_a 2\pi r_{IF} \frac{dr_{IF}}{d\theta} =$$

$$2\pi \sin\theta \left(\frac{S_*}{4\pi} - \frac{R_b^2 EM\alpha_H}{\cos\gamma} \right), \qquad (6)$$

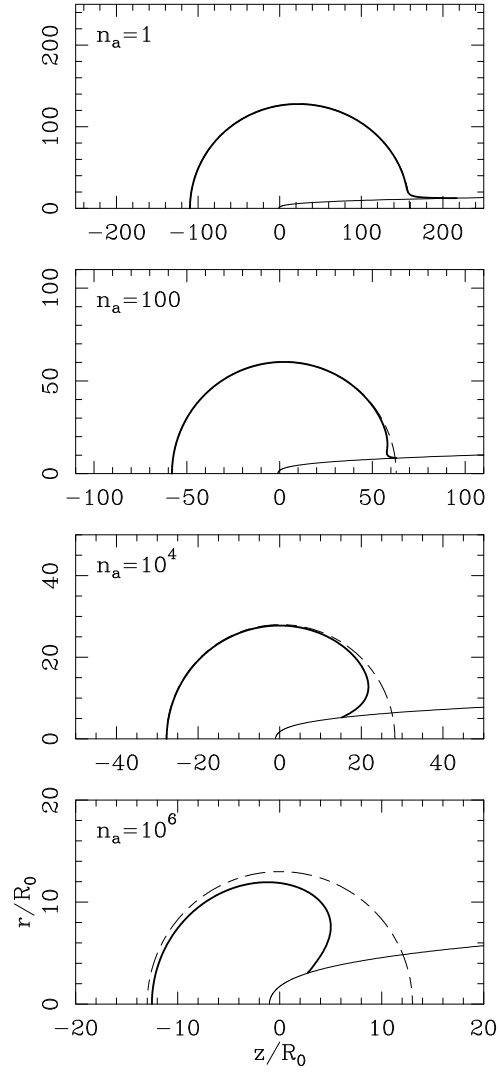where the terms in the equation represent:

Fig. 3. The same as Figure 2, but for the $v_a = 100\,\mathrm{km\,s}^{-1}$ models (see Table 1).

- first term on the left: recombination in the region with radii $R_b < R < R_{IF}$,

- second left term: flux of neutrals entering the ionization front,

- first term on the right: ionizing photon rate,

- second right term: recombinations within the bow shock shell,

per unit time within the solid angle between θ and $\theta + d\theta$. In this equation, $r_{IF} = R_{IF}\sin\theta$ is the cylindrical radius of the ionization front and α_H is the H recombination coefficient (we set $\alpha_H = 2.56 \times 10^{-13}\mathrm{cm}^3\,\mathrm{s}^{-1}$).
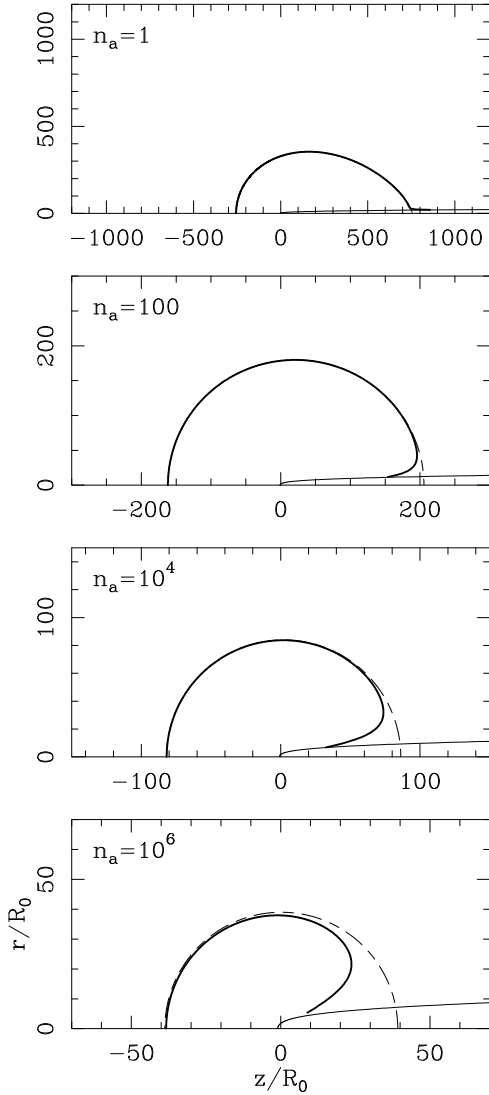
Fig. 4. The same as Figure 2, but for the $v_a = 200\,\mathrm{km\,s^{-1}}$ models (see Table 1).

Combining equations (3-6) we obtain the dimensionless equation:

$$\left(\frac{R_{IF}}{R_0}\right)^3 - \left[\frac{R_b}{R_0}(\theta)\right]^3 +$$

$$\chi\left(\frac{R_{IF}}{R_0}\right)\left[\frac{d(R_{IF}/R_0)}{d\theta}\sin\theta + \frac{R_{IF}}{R_0}\cos\theta\right] =$$

$$\left(\frac{R_S}{R_0}\right)^3 - \frac{3M_a^2}{2}G(\theta)\,, \tag{7}$$

where R_b/R_0 is given by equation (1),

$$M_a = \frac{v_a}{c_0} \tag{8}$$

is the Mach number of the impinging environment with respect to the isothermal sound speed of the photoionized gas,

$$R_S = \left(\frac{3S_*}{4\pi n_a^2\alpha_H}\right)^{1/3} \tag{9}$$

is the Strömgren radius and

$$\chi = \frac{3v_a}{n_a R_0 \alpha_H}\,, \tag{10}$$

where $n_a = \rho_a/\overline{m}$ is ion+atom environmental number density. The $G(\theta)$ function (describing the absorption of the bow shock shell as a function of θ) is given in Appendix A.

Our equation (7) is a generalization of equation (12) of Raga et al. (1997) (which has a dimensionless parameter $\xi = \chi R_0/R_s$) to the case of a cometary HII region with an inner stellar wind bow shock producing an appreciable absorption of the stellar ionizing photons.

For $\theta = 0$ from equation (7) we have:

$$\left(\frac{R_{IF,0}}{R_0}\right)^3 - 1 + \chi\left(\frac{R_{IF,0}}{R_0}\right)^2 =$$

$$\left(\frac{R_S}{R_0}\right)^3 - \frac{9M_a^2}{4}\,, \tag{11}$$

where we have used the fact that $G(0) = 3/2$ (see equation A17). This is a cubic equation which can be inverted (analytically or numerically) to obtain the on-axis radius $R_{IF,0}$ of the ionization front. This value can the be used to start a numerical integration of the ordinary differential equation (7) which then gives the shape $R_{IF}(\theta)$ of the ionization front.

Depending on the values of the parameters χ, R_S/R_0 and M_a, we find that equation (11) has either:

- one real root with $R_{IF,0}/R_0 > 1$, or

- no root satisfying this condition

This latter situation corresponds to the case in which the head of the bow shock traps the ionization front,

4. NUMERICAL RESULTS

As there is a considerable number of free parameters, a general exploration of the possible parameter space is lengthy (and also not very enlightening). We therefore choose to explore a limited range of parameters, which is appropriate for the case of a runaway O star passing through the plane of the Galaxy.

TABLE 1

MODELS FOR AN O7 STAR PASSING THROUGH THE GALACTIC PLANE

v_a[km/s]	n_a[cm^{-3}]	R_0[pc]	R_S/R_0	χ	$R_{IF,0}/R_0$
20	1	2.61	26.0	2.90	25.1
20	100	0.261	12.1	0.290	12.0
20	10^4	2.61e-2	5.60	2.90e-2	7.45
20	10^6	2.61e-3	2.60	2.90e-3	3.25
100	1	0.522	130.0	72.4	109.8
100	100	5.22e-2	60.35	7.24	58.0
100	10^4	5,22e-3	28.01	0.724	27.7
100	10^6	3.22e-4	13.00	7.24e-2	12.5
300	1	0.174	390.1	651.8	255.8
300	100	1.74e-2	181.1	65.18	161.8
300	10^4	1.74e-3	84.0	6.518	81.8
300	10^6	1.74e-4	39.0	0.6518	38.3

For the runaway O star, we choose a O7V star with wind velocity $v_w = 2500$ km s^{-1}, mass loss rate $\dot{M}_w = 4.5 \times 10^{-7} M_\odot$yr^{-1} and ionizing photon rate $S_* = 10^{49}$s^{-1}. For the streaming environment we choose three possible velocities ($v_a = 20$, 100 and 300 km s^{-1}) and four possible number densities ($n_a = 1$, 100, 10^4 and 10^6 cm^{-3}). The values of R_0, R_S/R_0 and χ corresponding to the chosen models are given in Table 1 (we do not list $M_a = v_a/10$ km s^{-1}).

For the combinations of these environmental velocities and densities we first calculate the axial standoff distance $R_{IF,0}$ of the ionization front from equation (11). The results of this exercise are given in Table 1. It is clear that for all of the chosen parameters the bow shock does not trap the ionization front, and that an external HII region is produced. The smaller HII region (relative to the size of the bow shock) is found for the $v_a = 20$ km s^{-1}, $n_a = 10^6$ cm^{-3} model, in which the on-axis radius of the ionization front is ≈ 3 times the bow shock radius (see Table 1).

With the $R_{IF}(\theta = 0) = R_{IF,0}$ initial condition, we integrate equation (7) to obtain the shape of the ionization front. The results for the $v_a = 20$ km s^{-1} models are shown in Figure 2, the ones for the $v_a = 100$ km s^{-1} models in Figure 3, and the results for the $v_a = 300$ km s^{-1} models in Figure 4,

Figures 2-4 show the stellar wind bow shock (equation 1), the ionization front R_{IF} obtained from equation (7), and the ionization front R_I obtained from equation (12) of Raga et al, (1997). R_I is the ionization front that would be obtained for a star producing a S_* ionizing photon rate, but with no wind (and therefore no stellar wind bow shock). In-

terestingly, in all but the $v_a = 20$ and 100 km s^{-1}, $n_a = 10^6$cm^{-3} model, no difference can be seen in the leading hemisphere of the HII region (i.e., for $z < 0$).

Substantial differences between R_{IF} and R_I can be seen in the trailing hemisphere. The absorption of ionizing photons by the bow shock wings and the lack of absorption within the stellar wind region lead to the formation of either:

- a thin downstream "horn" of ionized gas (in the $v_a = 20$ km s^{-1}, $n_a = 1 \rightarrow 10^4$cm^{-3} models, see Figure 2, and in the other two $n_a = 1$ models, see Figures 3 and 4),

- or a neutral, conical structure surrounding the extended bow shock wings (in all of the other models),

Except for the trailing region close to the bow shock wings, and except for the $v_a = 300$ km s^{-1}, $n_a = 1$ cm^{-3} model (top frame of Figure 4, which has a clearly non-spherical HII region), the ionization front always has an almost spherical shape, with a radius close to the Strömgren radius R_S for a star with S_* in a stationary medium of density n_a (given in the fourth column of Table 1). The sphere, however, is not centered on the position of the star, but on a position downstream of the star. This effect is described by the "$\chi \ll 1$ solution" of equation (13) of Raga et al. (1997), which to first order in χ corresponds to a sphere of radius R_S centered on a point with a downstream offset of $\chi R_0/3$ with respect to the position of the star.
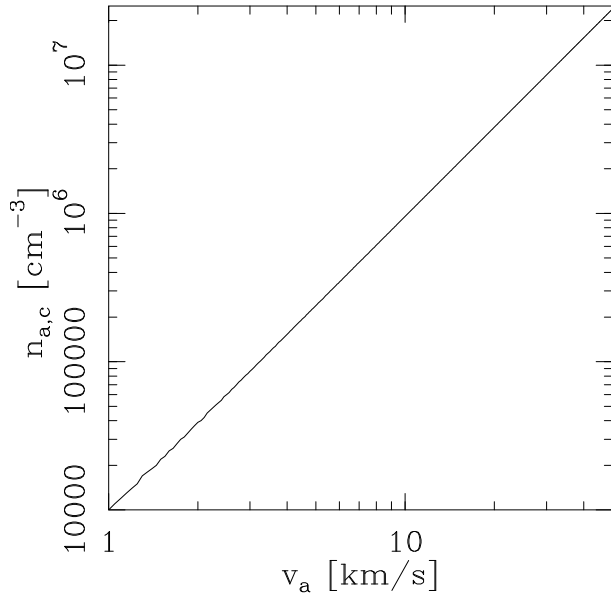
Fig. 5. Minimum environmental density $n_{a,c}$ (for capturing the ionization front) as a function of velocity v_a for the parameters of an O7V star (see the text).

5. DISCUSSION

Our exploration of the parameter space for the interaction of a runaway O7 star with the surrounding ISM shows that there is:

- a low density, high velocity regime (illustrated by our $v_a = 300$ km s^{-1}, $n_a = 1$ cm^{-3} model, see the top frame of Figure 4) in which an elongated HII region with a tear-drop shape is formed, with a characteristic size of several hundred times the on-axis radius of the the stellar wind bow shock,

- a high density, low velocity regime (illustrated by our $v_w = 20$ km s^{-1}, $n_a = 10^6$ cm^{-3} model, see the bottom frame of Figure 2) in which the photoionized environment is confined to a limited region around the head of the stellar wind bow shock,

- an "intermediate" regime (shown by all of the other models, see Figures 2-4), in which the HII region is approximately spherical, with a radius $\approx R_S$ and a small offset downstream from the stellar position, which intersects the stellar wind bow shock wings downstream of the star.

It is clear that we have not explored parameters for which the ionization front is trapped by the head of the stellar wind bow shock. Which parameters would be necessary for doing this? The condition for

ionization front capture at the head of the bow shock can be obtained by setting $R_{IF,0} = R_0$ in equation (11), which gives:

$$\left(\frac{R_S}{R_0}\right)^3 = \chi + \frac{9M_a^2}{4}, \qquad (12)$$

where R_S is given by equation (9), R_0 by equation (2), M_a by equation (8) and χ by equation (10) as functions of the physical parameters of the flow. If we fix the stellar parameters for an O7V star, the remaining free parameters are the density and velocity of the streaming environment. Equation (12) then gives us the minimum environmental density $n_{a,c}$ as a function of velocity v_a necessary for the ionization front to be captured by the head of the bow shock. The results of this exercise are shown in Figure 5.

We see that for the $v_a = 1 \to 40$ km s^{-1} range shown in Figure 5, the critical density is in the $n_{a,c} \propto v_a^{1/2}$ regime obtained from equation (12) for $\chi \ll 1$. It is clear that for $v_a \geq 1$ km s^{-1}, large environmental densities are required in order for the bow shock to capture the ionization front!

For $v_a > 10$ km s^{-1} stellar motions, $n_{a,c} > 10^7$ cm^{-3} environmental densities are required, so that it is unlikely that one will ever find such objects with ionization fronts captured by the stellar wind bow shocks. For lower values of v_a, one could have captured ionization fronts provided that the objects travel within a dense molecular cloud (of densities $\approx 10^5 \to 10^7$ cm^{-3}, see Figure 5).

We are, of course, now talking about compact/ultracompact HII regions within dense molecular clouds, produced by massive stars with velocities of a few km/s with respect to the surrounding cloud. Interestingly, as we see in Figure 5, we could also have O stars with $v_a = 1 \to 10$ km s^{-1} with bow shocks that do not capture the ionization fronts. This parameter regime is interesting because it is not correctly described by our present model.

For $v_a < 10$ km s^{-1}, the steady bow shock+HII region configuration (for a case in which the IF is not captured by the bow shock) will have a motion through the neutral environment that is subsonic with respect to the $c_0 \approx 10$ km s^{-1} isothermal sound speed of the ionized gas. Such an ionization front will have a strong hydrodynamical effect, driving a shock wave ahead of it into the neutral environment. The post-shock material will be almost at rest with respect to the star, and therefore will not shock again before reaching the contact discontinuity against the stellar wind.

The flow configuration will then have an inner shock involving the stellar wind, and an outer shock

surrounding an extended HII region. This outer bow shock will be somewhat peculiar, since all of the post-shock flow (even far along the bow shock wings) will be subsonic (because the pre-shock flow is subsonic with respect to c_0). Therefore, the post-bow shock flow will not have the typical division between a compact axial subsonic region and an extended supersonic region farther away from the flow axis.

In a future paper we will continue with a study of this interesting regime (already explored by Arthur & Hoare 2006) with axisymmetric gasdynamic+radiative transfer simulations. Clearly, the codes needed to do this have already been fully developed (see, e.g., Mackey et al. 2021).

APPENDIX

A. ANGULAR DEPENDENCE OF THE EMISSION MEASURE

In this appendix we give the functions determining the angular dependence of the emission measure of the thin shell solution of equation (1). The functions that we give here correspond to the results of Cantó et al. (2005) evaluated for the case of a uniform environment,

We first give the functions used in equation (4):

$$f_a(\theta) = \frac{[R'\cos\theta + (dR'/d\theta)\sin\theta]^2}{R'^2 + (dR'/d\theta)^2}, \quad \text{(A13)}$$

$$f_w(\theta) = \frac{R'^2}{R'^2 + (dR'/d\theta)^2}, \quad \text{(A14)}$$

$$g_\sigma(\theta) = \frac{2\left[(v_a/v_w)(1-\cos\theta) + R'^2\sin^2\theta/2\right]^2}{R'\sin\theta\sqrt{(\theta - \sin\theta\cos\theta)^2 + (1-R'^2)^2\sin^4\theta}}, \quad \text{(A15)}$$

where $R' = R_b/R_0$ is given by equation (1) and

$$\frac{dR'}{d\theta} = \frac{\sqrt{3}\csc\theta\,\left[(3\csc^2\theta - 2)\theta - 3\operatorname{ctg}\theta\right]}{2\sqrt{1-\theta\operatorname{ctg}\theta}}. \quad \text{(A16)}$$

We should note that $g_v(\theta)$ has a dependence on the v_a/v_w velocity ratio. For the case of a runaway O star, $v_a/v_w \ll 1$, and we can therefore put $v_a/v_w \approx 0$ in equation (A15) and eliminate this dependence.

Finally, the $G(\theta)$ function of equation (7) is:

$$G(\theta) = \left(\frac{R_b}{R_0}\right)^2 [f_a(\theta) + f_w(\theta)]\, g_\sigma(\theta)\,\sec\gamma, \quad \text{(A17)}$$

where γ is the angle between the normal to the bow shock and the direction towards the star (see Figure 1). This angle can be calculated through:

$$\cos\gamma = \sin(\theta + \alpha), \quad \text{(A18)}$$

where the slope of the bow shock shape is given by

$$\tan\alpha = \frac{2\sin\theta(\sin 2\theta - 2\theta)}{12\theta\cos\theta - 9\sin\theta - \sin 3\theta}. \quad \text{(A19)}$$

REFERENCES

Arthur, S. J. & Hoare, M. G. 2006, ApJS, 165, 283, https://doi.org/10.1086/503899

Cantó, J., Raga, A. C., & Wilkin, F. P. 1996, ApJ, 469, 729, https://doi.org/10.1086/177820

Cantó, J., Raga, A. C., & González, R. 2005, RMxAA, 41, 101

Cruz-González, C., Recillas-Cruz, E., & Costero, R. 1974, RMxAA, 1, 211

Dyson, J. E. 1975, Ap&SS, 35, 299, https://doi.org/10.1007/BF00636999

Mac Low, M. M., Van Buren, D., Wood, D. O. S., & Churchwell, E. 1991, ApJ, 369, 395, https://doi.org/10.1086/169769

Mackey, J., Green, S., Moutzouri, M., et al. 2021, MNRAS, 504, 983, https://doi.org/10.1093/mnras/stab781

Mackey, J., Langer, N., & Gvaramadze, V. V. 2013, MNRAS, 436, 859, https://doi.org/10.1093/mnras/stt1621

Meyer, D. M. -A., Mignone, A., Kuiper, R., Raga, A. C., & Kley, W. 2017, MNRAS, 464, 3229, https://doi.org/10.1093/mnras/stw2537

Meyer, D. M.-A., Mackey, J., Langer, N., et al. 2014, MNRAS, 444, 2754, https://doi.org/10.1093/mnras/stu1629

Noriega-Crespo, A., Van Buren, D., & Dgani, R. 1997, AJ, 113, 780, https://doi.org/10.1086/118298

Raga, A. C., Noriega-Crespo, A., Cantó, J., et al. 1997, RMxAA, 33, 73

Rasiwala, M. 1969, A&A, 1, 431

Stevens, I. R., Blondin, J. M., & Pollock, A. M. T. 1992, ApJ, 386, 265, https://doi.org/10.1086/171013

Thuan, T. X. 1975, ApJ, 198, 307, https://doi.org/10.1086/153607

Van Buren, D., Noriega-Crespo, A., & Dgani, R. 1995, AJ, 110, 2914, https://doi.org/10.1086/117739

Van Buren, D., Mac Low, M.-M., Wood, D. O. S., & Churchwell, E. 1990, ApJ, 353, 570, https://doi.org/10.1086/168645

Wilkin, F. P. 1996, ApJ, 459, 31, https://doi.org/10.1086/309939

J. Cantó: Instituto de Astronomía, Universidad Nacional Autónoma de México, Ap. 70-468, 04510 CDMX, México.

A. Noriega-Crespo: Space Telescope Science Institute, 3700 San Martin Dr., Baltimore, MD 21211, USA.

A. C. Raga: Instituto de Ciencias Nucleares, Universidad Nacional Autónoma de México, Ap. 70-543, 04510 CDMX, México (raga@nucleares.unam.mx).